Chemical Science

ROYAL SOCIETY OF CHEMISTRY

EDGE ARTICLE

View Article Online
View Journal | View Issue

Cite this: *Chem. Sci.*, 2025, **16**, 4366

All publication charges for this article have been paid for by the Royal Society of Chemistry

Received 29th December 2024
Accepted 23rd January 2025

DOI: 10.1039/d4sc08771b

rsc.li/chemical-science

Zn(II)-driven impact of monomeric transthyretin on amyloid-β amyloidogenesis†

Yelim Yi,[a] Bokyung Kim,[b] Mingeun Kim,[a] Young Ho Ko,[c] Jin Hae Kim*[b] and Mi Hee Lim*[a]

Extracellular accumulation of amyloid-β (Aβ) peptides in the brain plays a significant role in the development of Alzheimer's disease (AD). While the co-localization and interaction of proteins and metal ions with Aβ in extracellular milieu are established, their precise pathological associations remain unclear. Here we report the impact of Zn(II) on the anti-amyloidogenic properties of monomeric transthyretin (M-TTR), which coexists spatially with Aβ and Zn(II) in extracellular fluids. Our findings demonstrate the Zn(II)-promoted ternary complex formation involving M-TTR, Aβ, and Zn(II) as well as M-TTR's proteolytic activity towards Aβ. These interactions decrease the inhibitory effect of M-TTR on the primary nucleation process of Aβ as well as its ability to improve cell viability upon treatment of Aβ. This study unveils the variable activities of M-TTR towards Aβ, driven by Zn(II), providing insights into how metal ions influence the entanglement of M-TTR in the Aβ-related pathology linked to AD.

Introduction

Alzheimer's disease (AD), the most common form of dementia, is a leading cause of death and currently lacks a cure.[1] In the brains of AD patients, the formation of extracellular deposits occurs as a consequence of the conversion of amyloid-β (Aβ) peptides into toxic oligomers and fibrils.[2,3] To release the burden of these aggregates in the brain, proteins available in extracellular fluids sequester cerebral Aβ species, compensating for the pathological cascade of Aβ by protein–protein interactions.[4,5] Transthyretin (TTR) is a major extracellular protein identified as an Aβ-binding protein in the cerebrospinal fluid (CSF) and serves as a carrier of Aβ from the brain to the blood.[6–10] Previous studies have demonstrated the ability of TTR to ameliorate neuropathologic manifestations of AD *in vivo*,[6] and the decrease in its levels in extracellular fluids from AD patients further supports its neuroprotective function in the disease pathology.[11–13]

Additionally, highly concentrated metal ions have been detected in Aβ aggregate deposits.[14–19] These metal ions bind to Aβ peptides, forming metal–Aβ complexes, which alters the aggregation and toxicity of Aβ.[14–26] In the case of TTR, the diseased states lead to the dissociation of its native homotetrameric structure into aggregation-prone monomers (M-TTR), rendering it vulnerable to metal coordination by exposing additional surfaces.[27–31] *Ex vivo* observations have denoted the prevalence of M-TTR in the CSF and its aggregates enriched with Zn(II), implying the capacity of M-TTR to interact with Zn(II).[32–34] Despite these findings, the connection of this interactive network involving Aβ, M-TTR, and Zn(II) to the pathology of AD remains elusive. Herein, we questioned whether M-TTR exhibits anti-amyloidogenic activity against Aβ in the presence of Zn(II). Thus, we determined the direct binding between M-TTR and Aβ under Zn(II)-present conditions, with the subsequent variation in the structure of Aβ. Furthermore, the influence of M-TTR on the aggregation and toxicity profiles of Aβ in the presence of Zn(II) was probed.

Results and discussion

Using a TTR mutant, Phe87Met/Leu110Met TTR, which mainly remains monomeric (M-TTR) in an aqueous solution at neutral pH and room temperature,[35,36] we explored the impact of M-TTR on the aggregation of Aβ in the presence of Zn(II), as illustrated in Fig. 1a and b. We first monitored the aggregation kinetics of $Aβ_{40}$, which is the most prevalent Aβ in the CSF,[37] in the presence of Zn(II) upon treatment of various concentrations of M-TTR by the thioflavin-T (ThT) assay that enables to quantify the amount of β-sheet-containing aggregates.[21,38] As shown in Fig. 1c, the ThT fluorescence intensity for the entire aggregation process of $Aβ_{40}$ treated with Zn(II) remarkably lowered with the addition of M-TTR. M-TTR incubated with or without Zn(II) did not produce ThT-detectable aggregates (Fig. S1†). This manifests the inhibition of M-TTR on the formation of ThT-reactive

[a]*Department of Chemistry, Korea Advanced Institute of Science and Technology (KAIST), Daejeon 34141, Republic of Korea. E-mail: miheelim@kaist.ac.kr*

[b]*Department of New Biology, Daegu Gyeongbuk Institute of Science and Technology (DGIST), Daegu 42988, Republic of Korea. E-mail: jinhaekim@dgist.ac.kr*

[c]*Center for van der Waals Quantum Solids, Institute for Basic Science, Pohang 37673, Republic of Korea*

† Electronic supplementary information (ESI) available: Experimental section, Table S1 and Fig. S1–S20. See DOI: https://doi.org/10.1039/d4sc08771b

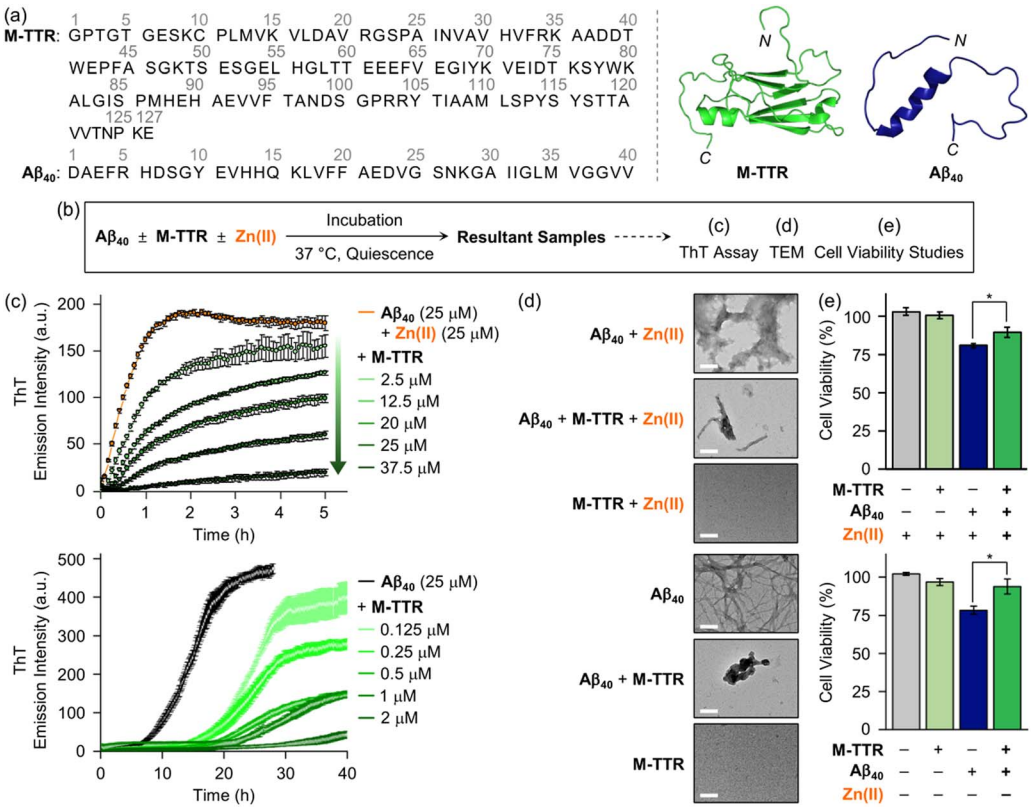

Fig. 1 Anti-amyloidogenic activity of M-TTR against $A\beta_{40}$ with and without Zn(II). (a) Amino acid sequences and structures of M-TTR and $A\beta_{40}$ determined by NMR spectroscopy (PDB 2NBO[36] for M-TTR; PDB 2LFM[40] for $A\beta_{40}$). (b) Scheme of the aggregation studies. (c) Aggregation kinetics of $A\beta_{40}$ in the presence of M-TTR with (top) and without (bottom) Zn(II) monitored by the ThT assay. Conditions: $[A\beta_{40}] = 25$ μM; [M-TTR] = 0.125–37.5 μM; $[ZnCl_2] = 25$ μM; 20 mM HEPES, pH 7.4, 150 mM NaCl; 37 °C; quiescent conditions; $\lambda_{ex} = 440$ nm; $\lambda_{em} = 490$ nm. The error bars denote s.e.m. for $n = 9$ examined over three independent experiments. (d) Morphologies of the resultant peptide and protein aggregates detected by TEM. Conditions: $[A\beta_{40}] = 25$ μM; [M-TTR] = 25 μM; $[ZnCl_2] = 25$ μM; 20 mM HEPES, pH 7.4, 150 mM NaCl; 37 °C; 24 h incubation; quiescent conditions. Scale bars, 200 nm. (e) Survival of the cells upon treatment of $A\beta_{40}$ incubated with M-TTR in the presence (top) and absence (bottom) of Zn(II). The viability of 5Y cells, analyzed by the MTT assay, was calculated, compared to that with an equivalent amount of the buffered solution. Conditions: $[A\beta_{40}] = 25$ μM; [M-TTR] = 25 μM; $[ZnCl_2] = 25$ μM. The error bars denote s.e.m. for $n = 6$ examined over three independent experiments. All statistical significance was determined by a two-sided unpaired Student's t-test. *$P < 0.05$.

$A\beta_{40}$ aggregates in the presence of Zn(II). Given the sub-equimolar, equimolar, and supra-equimolar ratios of M-TTR to Zn(II) under physiological conditions,[32,33,39] these results suggest that the inhibitory effect of M-TTR on the assembly of Zn(II)–$A\beta_{40}$ may vary in biological environments. Such modulative effect of M-TTR on $A\beta_{40}$ aggregation with Zn(II) was further confirmed by transmission electron microscopy (TEM). As illustrated in Fig. 1d, $A\beta_{40}$ treated with M-TTR in the presence of Zn(II) exhibited a mixture of smaller amorphous aggregates and chopped fibrils, distinct from larger aggregates observed for Zn(II)-bound $A\beta_{40}$ [Zn(II)–$A\beta_{40}$]. For the samples of M-TTR, no aggregates were visible under Zn(II)-treated conditions. Clearly, these results indicate that M-TTR can significantly redirect the aggregation of $A\beta_{40}$ in the presence of Zn(II). The toxicity of the resultant samples in human neuroblastoma SH-SY5Y (5Y) cells was then evaluated by the MTT assay [MTT = 3-(4,5-dimethylthiazol-2-yl)-2,5-diphenyltetrazolium bromide]. $A\beta_{40}$ aggregates produced with M-TTR and Zn(II) were observed to be less cytotoxic by *ca.* 10%, compared to those formed only with Zn(II), under our experimental conditions (Fig. 1e). The Zn(II)-treated M-TTR sample was not significantly toxic. Collectively, M-TTR in the presence of Zn(II) reduces the formation of toxic $A\beta_{40}$ aggregates. It should be noted that the hydrolytic products of $A\beta_{40}$ generated in the presence of M-TTR and Zn(II) may contribute to the cell viability (*vide infra*). The effects of M-TTR without Zn(II) on $A\beta_{40}$ aggregation and toxicity were consistent with those observed in the previous reports,[8,41–43] showing more discernible anti-amyloidogenic activity relative to that under Zn(II)-treated conditions (Fig. 1). Overall, our results indicate that Zn(II) impairs M-TTR's ability to control the aggregation of $A\beta_{40}$ and improve the cell viability upon treatment of $A\beta_{40}$. Specifically, a *ca.* 4% decrease in cell viability was observed when cells were treated with Zn(II)–$A\beta_{40}$ incubated with M-TTR, compared to those added with $A\beta_{40}$ and M-TTR without Zn(II).

Confirming the decrease in anti-amyloidogenic activity of M-TTR in the presence of Zn(II), we identified the specific microscopic step in the assembly of $A\beta_{40}$ influenced by M-TTR under Zn(II)-added conditions. We initially analyzed the microscopic processes in the aggregation mechanisms of Zn(II)–$A\beta_{40}$ without

M-TTR by global fitting of previously delineated mathematical models for the protein assembly[44] to experimental data sets. As shown in Fig. S2,† macroscopic aggregation curves for various concentrations of $A\beta_{40}$ with equimolar Zn(II) were obtained by the ThT assay. Based on their normalized curves depicted in Fig. 2a, the values of half-time ($t_{1/2}$), the time at which the ThT fluorescence intensity reaches half of its maximum value, were plotted against the peptide concentration on a double logarithmic scale. A resultant linear plot denotes that a single aggregation mechanism is dominant[44,45] for the self-assembly of Zn(II)–$A\beta_{40}$ under our experimental conditions. Global fitting of various kinetic models to the curves revealed that an aggregation model involving primary nucleation and elongation steps (*i.e.*, nucleation–elongation model)[44] well-described the experimental data (Fig. 2a and Table S1†). A reasonable global fit to the data was also acquired if the secondary nucleation step was included in the aforementioned model (Fig. S3†). To evaluate whether the secondary nucleation process is entailed in the assembly of Zn(II)–$A\beta_{40}$, we performed additional experiments with seeds, preformed $A\beta_{40}$ aggregates generated in the presence of Zn(II) (Fig. S4†). According to previously reported studies, the addition of a relatively small amount of seeds (*e.g.*, up to 5% v/v) can dramatically increase the aggregation rate of Aβ, representing the assembly with substantial intermediation of the secondary nucleation step.[44,46,47] Our results, however, showed similar $t_{1/2}$ values of Zn(II)–$A\beta_{40}$ aggregation with various quantities of seeds up to 5% v/v. Therefore, the primary nucleation and elongation processes predominantly participate in the aggregation of Zn(II)–$A\beta_{40}$, without significant involvement of the secondary nucleation step.

Next, as presented in Fig. 2b, the inhibitory effect of M-TTR on the aggregation of $A\beta_{40}$ in the presence of Zn(II) was quantitatively analyzed through global fitting of the nucleation–elongation model[44] to the experimental data shown in Fig. 1c. As a result, the combined rate constants of primary nucleation (k_n) and elongation (k_+), k_+k_n values, gradually decreased with

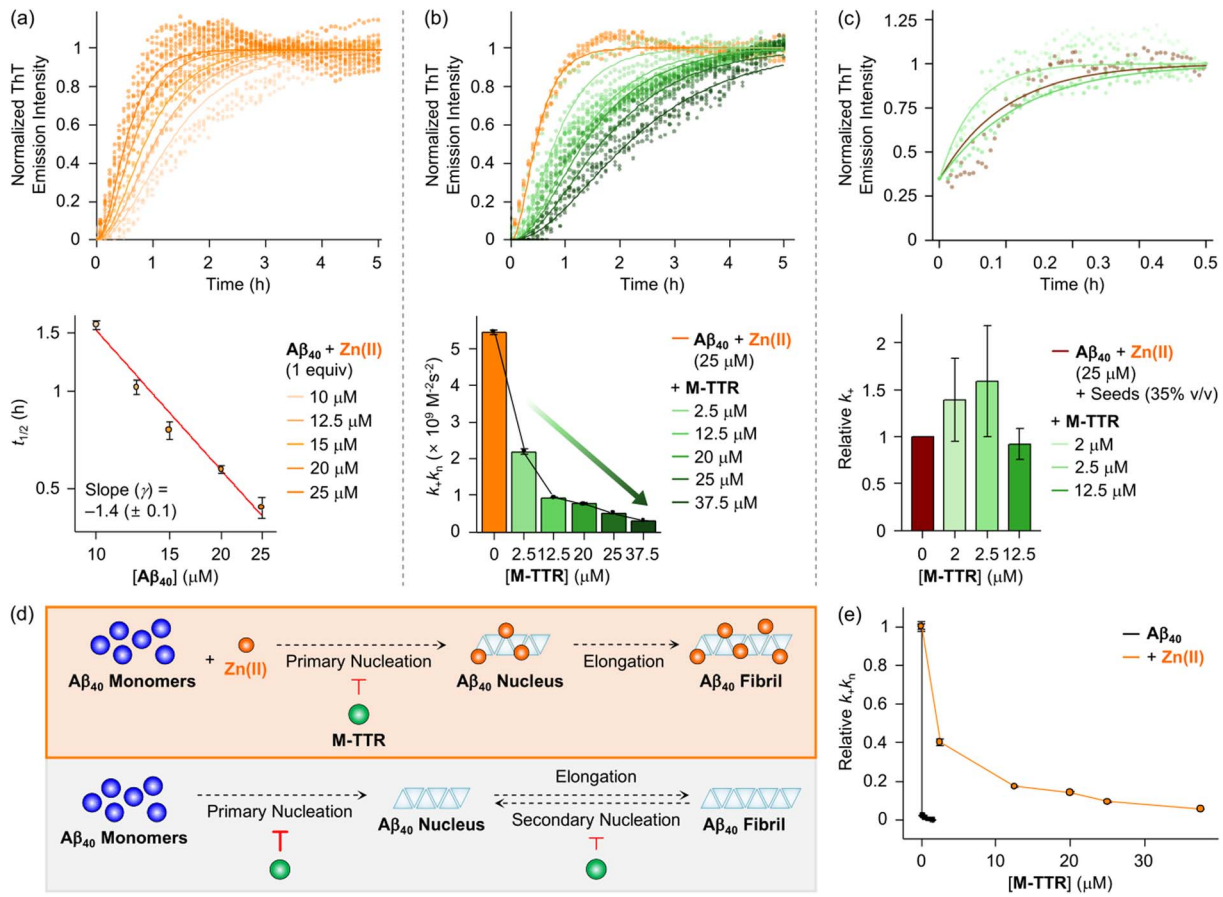

Fig. 2 Aggregation kinetics of Zn(II)-added $A\beta_{40}$ with and without M-TTR analyzed by the ThT assay. (a) Normalized aggregation curves of $A\beta_{40}$ in the presence of equimolar Zn(II) (top) and the $t_{1/2}$ value of each curve plotted against [$A\beta_{40}$] for obtaining scaling exponent (γ) (bottom). The nucleation–elongation model was well-fitted to the data (top; solid lines). (b) Normalized aggregation curves of Zn(II)–$A\beta_{40}$ in the presence of M-TTR (top) and the combined rate constant, k_+k_n, plotted against [M-TTR] (bottom). The nucleation–elongation model with the variations in k_+k_n values was well-fitted to the data (top; solid lines). (c) Normalized aggregation curves of Zn(II)–$A\beta_{40}$ with seeds in the absence and presence of M-TTR (top; mean residual error, 0.0078) and the relative k_+ values plotted against [M-TTR] (bottom). Solid lines are the fits of Zn(II)–$A\beta_{40}$ aggregation profiles upon treatment of various [M-TTR] with the alteration in k_+. (d) Schematic representation of $A\beta_{40}$ aggregation with and without Zn(II) (black lines) affected by M-TTR (red lines). (e) Change in the relative k_+k_n values of Zn(II)-added and -unadded $A\beta_{40}$ aggregation plotted as a function of [M-TTR].

increasing the concentration of M-TTR, showing a reduction by *ca.* 90% with 1.5 equiv. of M-TTR. This implies the ability of M-TTR to impede either primary nucleation, elongation, or both of Zn(II)–Aβ_{40} assembly. To probe which of the microscopic steps is mainly influenced by M-TTR, Zn(II)–Aβ_{40} aggregation with M-TTR was observed in the presence of 35% v/v seeds, which can induce elongation-dominant aggregation (Fig. S5†).[44,46,47] Fig. 2c illustrates that M-TTR did not noticeably affect the aggregation kinetics of Zn(II)–Aβ_{40} with seeds exhibiting similar k_+ values. This demonstrates that M-TTR predominantly hampers the primary nucleation process, rather than the elongation step, in the self-assembly of Zn(II)–Aβ_{40}. Collectively, as summarized in Fig. 2d, in the presence of Zn(II), Aβ_{40} assembles *via* the combination of primary nucleation and elongation processes. Intriguingly, M-TTR can dominantly retard the primary nucleation of Zn(II)–Aβ_{40}.

Similar experiments were conducted with Zn(II)-untreated samples (Fig. S6–S10 and Table S1†). Metal-free Aβ_{40} aggregation involves primary nucleation, elongation, and secondary nucleation catalyzed by the surface of preformed aggregates that can be saturated by incoming peptide species (Fig. 2d), consistent with previously reported results.[48] The nucleation steps of metal-free Aβ_{40} (particularly, primary nucleation), following previous reports,[8,43] can be primarily affected by the introduction of M-TTR. Since the elongation steps for both Zn(II)-treated and metal-free Aβ_{40} were not considerably perturbed by M-TTR, the change in k_+k_n values upon addition of M-TTR can be interpreted as M-TTR-triggered alteration in the primary nucleation of Aβ_{40}. As shown in Fig. 2e, the k_+k_n value of Zn(II)-added Aβ_{40} was lowered by M-TTR, with an even greater reduction observed under Zn(II)-unadded conditions. In particular, the addition of M-TTR (2.5 μM) reduced the k_+k_n value of Zn(II)–Aβ_{40} by *ca.* 60%, whereas the value was lowered by *ca.* 100% in the presence of M-TTR (1.5 μM) under Zn(II)-untreated conditions. Overall studies manifest that while Zn(II) diminishes the inhibitory effect of M-TTR on the formation of primary nuclei of Aβ_{40}, it does not completely eliminate the effect.

To elucidate how Zn(II) decreases the anti-amyloidogenic activity of M-TTR towards Aβ_{40}, we investigated Zn(II)-binding properties of M-TTR in the absence and presence of Aβ_{40}. Given the limited spectral changes of M-TTR mixed with Zn(II), the dissociation constant (K_d) was estimated through competitive Zn(II) titration experiments using Zincon (2-carboxy-2′-hydroxy-5′-sulfoformazyl-benzene monosodium salt), an indicator that shows electronic absorption (Abs) at 618 nm upon Zn(II) coordination with a K_d value in the micromolar range (Fig. S11†).[49] As shown in Fig. S12a,† electronic Abs spectra exhibited no noticeable variation in Abs at 618 nm when the solution of M-TTR and Zincon was titrated with sub-equimolar Zn(II). In contrast, the addition of supra-equimolar Zn(II) notably elevated the Abs at 618 nm. These observations indicate that M-TTR can bind to 1 equiv. of Zn(II) with a binding affinity similar to or greater than that of Zincon. Considering that M-TTR includes three Zn(II)-binding sites,[33] the affinity of M-TTR binding to Zn(II) greater than 1 equiv. could be weaker than that of Zincon. Based on the spectral changes at 618 nm, the apparent K_d value for Zn(II)–M-TTR was calculated to be in a micromolar range. Given the Hill coefficient (n) of 0.74 (±0.04), as depicted in Fig. S12b,† this apparent K_d value indicates the involvement of at least two Zn(II)-binding events in M-TTR.

Furthermore, we probed the interaction of Aβ_{40} with M-TTR in the presence of Zn(II) by two-dimensional ^{1}H–^{15}N heteronuclear single quantum coherence nuclear magnetic resonance (2D ^{1}H–^{15}N HSQC NMR) spectroscopy, as presented in Fig. 3a and S13.† The discernible alteration in the NMR signals of amino acid residues in or near the *N*-terminal region of ^{15}N-labeled Aβ_{40} was observed upon addition of Zn(II) (Fig. 3a, top). Specifically, the peaks of some amino acid residues (*e.g.*, Arg5, Asp7, Ser8, and Val12) adjacent to the Zn(II)-binding site in Aβ^{14-19} disappeared, suggestive of Zn(II) binding to Aβ_{40}.[50,51] Interestingly, mixing M-TTR with the solution of ^{15}N-labeled Aβ_{40} with Zn(II) restored the vanished peaks to certain extents. This reveals that M-TTR can partially disrupt Zn(II) binding to Aβ_{40}. The comparable Zn(II)-binding affinities of Aβ^{14-18} and M-TTR (Fig. S12†) in the micromolar range support this competitive Zn(II) binding of M-TTR with Aβ_{40}. Prior studies described that Zn(II) coordination to M-TTR increases the structural flexibility of the region flanking α-helix (Fig. 1a).[33] Given that the helical region of M-TTR can be involved in the association with Aβ,[8,42,52,53] when it interacts with Zn(II) from Zn(II)–Aβ_{40}, its subsequent structural perturbation could impact the binding and reactivity with Aβ_{40}. The spectra further displayed that Zn(II) moderately induced the chemical shift perturbations (CSPs) of peaks corresponding to Ser8, Glu11, Val12, Gln15, Phe20, and Val24 in ^{15}N-labeled Aβ_{40} treated with M-TTR (Fig. 3a, middle). Without Zn(II), the modest CSPs for ^{15}N-labeled Aβ_{40} at Gln15, Val24, and Lys28 were revealed upon treatment of M-TTR (Fig. 3a, bottom). These may indicate the Zn(II)-directed ternary complexation among M-TTR, Zn(II), and Aβ_{40}.

Investigations employing electrospray ionization-mass spectrometry (ESI–MS) further corroborate these findings. As depicted in Fig. 3b, a peak at *ca.* 2011 m/z, assigned to be a 9+-charged ion, appeared when Aβ_{40} was incubated with M-TTR and Zn(II). Tandem MS (ESI–MS^2) analysis with applying collision-induced dissociation (CID) energy to this peak resulted in multiply charged peaks corresponding to $[\text{M-TTR} + \text{Zn(II)}]^{7+}$ and $[\text{A}\beta_{40} + \text{Zn(II)}]^{2+}$, indicating a ternary complexation of Aβ_{40} with M-TTR and Zn(II). This metal-assisted ternary complexation associated with Aβ was proposed to alter the aggregation.[54] This may support the contribution of Zn(II) to the suppressive effect of M-TTR on the assembly of Aβ_{40} accompanied by the perturbation in Aβ_{40}'s primary nucleation (Fig. 2d). It should be noted that the Zn(II)-binding affinity of M-TTR in the presence of Aβ could not be accurately determined under our experimental conditions, likely due to the formation of a ternary complex. Without Zn(II) treatment, 8+-charged (*ca.* 2263 m/z) and 10+-charged (*ca.* 2243 m/z) peaks appeared (Fig. S14†), corresponding to heterodimers and heterotrimers comprised of M-TTR with monomeric and dimeric Aβ_{40}, respectively.[41] The direct interaction between the aggregates of Aβ_{40} and M-TTR was also monitored by cross-linking experiments. Glutaraldehyde, a well-known cross-linking reagent, covalently conjugated the peptide and protein aggregates

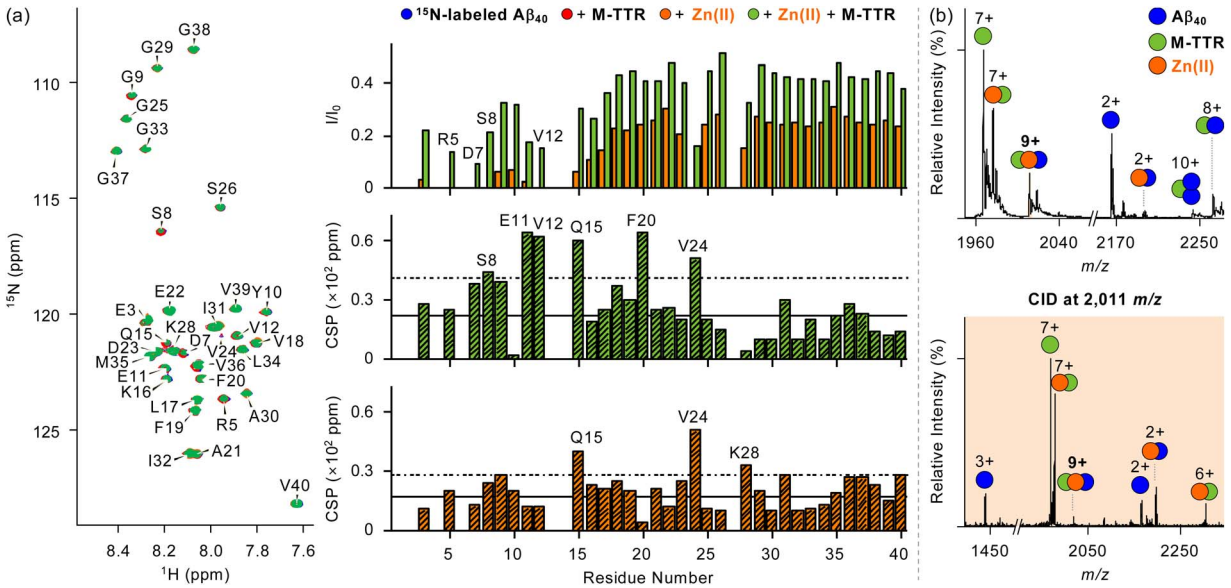

Fig. 3 Interaction of M-TTR with Aβ$_{40}$ in the presence of Zn(II). (a) 2D ^{1}H–^{15}N HSQC NMR (850 MHz) spectra of ^{15}N-labeled Aβ$_{40}$ treated with either M-TTR, Zn(II), or both. (Top) The peak intensity ratios (I/I_0) of amino acid residues in ^{15}N-labeled Aβ$_{40}$ upon treatment of Zn(II) with (green) and without (orange) M-TTR were calculated. The CSPs of amino acid residues in (middle) M-TTR-added ^{15}N-labeled Aβ$_{40}$ upon addition of Zn(II) and (bottom) ^{15}N-labeled Aβ$_{40}$ upon treatment of M-TTR were obtained. The average of CSPs and the sum of the average and one standard deviation are indicated with solid and dashed lines, respectively. Conditions: [^{15}N-labeled Aβ$_{40}$] = 35 μM; [M-TTR] = 35 μM; [$ZnCl_2$] = 35 μM; 50 mM HEPES, pH 7.4; 7% v/v D_2O; 10 °C. (b) M-TTR binding to Aβ$_{40}$ in the presence of Zn(II) monitored by ESI–MS and ESI–MS^2. Charge states are marked above the peaks in the spectra. Conditions: [Aβ$_{40}$] = 100 μM; [M-TTR] = 100 μM; [$ZnCl_2$] = 100 μM; 20 mM ammonium acetate, pH 7.4; 37 °C; 3 h incubation; quiescent conditions. The samples were diluted 10-fold before injection into the mass spectrometer. The measurements were conducted in triplicate.

generated from the aggregation studies (Fig. 1b).[42,55] The size distribution of the resultant samples was analyzed by sodium dodecyl sulfate–polyacrylamide gel electrophoresis (SDS–PAGE) with western blotting using anti-Aβ (6E10) and anti-TTR antibodies (Fig. S15†). As shown in Fig. S16,† different from the samples of either Aβ$_{40}$ or M-TTR with and without Zn(II), new bands between 35 kDa and 48 kDa were displayed for Aβ$_{40}$ samples incubated with M-TTR under both Zn(II)-treated and -untreated[41] conditions. These observations substantiate that dimeric Aβ$_{40}$ can form heterotetramers with dimeric M-TTR with and without Zn(II).

Moving forward, the impact of the direct interaction between Aβ$_{40}$ and M-TTR in the presence of Zn(II) on the structure of Aβ$_{40}$ was assessed through ESI–MS studies. As depicted in Fig. 4, after incubating Aβ$_{40}$ with M-TTR and Zn(II) for 24 h, new peaks at *ca.* 850 *m*/*z* and *ca.* 1325 *m*/*z* were detected, distinguishing them from the spectra obtained without Zn(II) treatment (Fig. S17†). ESI–MS^2 in conjunction with CID characterized these peaks as Aβ$_{1-14}{}^{2+}$ and Aβ$_{15-40}{}^{2+}$ fragments, respectively. These fragments were not generated with Aβ$_{40}$ samples relatively shortly incubated with M-TTR and Zn(II) for 3 h (Fig. S18†) and, thus, they could not be detected in the 2D ^{1}H–^{15}N HSQC NMR spectrum of Aβ$_{40}$ with M-TTR in the presence of Zn(II) (Fig. 3). According to prior studies regarding the proteolytic competence of TTR against peptides or proteins induced by Zn(II),[56,57] these fragmentations could result from the proteolytic activity of M-TTR in the presence of Zn(II). The binding of truncated Aβ with full-length ones can accelerate the generation of primary nuclei.[58] Thus, proteolytic reactions catalyzed by M-TTR with Zn(II) could decrease the inhibitory effect of M-TTR on the primary nucleation process of Aβ$_{40}$ (Fig. 2d). In particular, Aβ$_{15-40}$ was suggested as an amyloid core segment capable of interacting with itself and the full-length of Aβ. While Aβ$_{15-40}$ has intrinsic amyloidogenic properties to form toxic aggregates, it can redirect the assembly of full-length Aβ$_{40}$ into non-fibrillar and less toxic aggregates.[59] These aggregates may contribute to the observed cell viability upon treatment with the Aβ$_{40}$ sample incubated with M-TTR and Zn(II) (Fig. 1e). In the case of Aβ$_{1-14}$, as the least hydrophobic domain of Aβ$_{40}$,[60] it is less likely to interact with itself or Aβ$_{40}$ to form amyloids; however, previous studies reported that the *N*-terminal regions of Aβ, including Aβ$_{1-14}$, could interact with cell receptors (*e.g.*, glutamate or *N*-methyl-D-aspartate receptors), potentially leading to cytotoxicity.[60] Thus, the generation of Aβ$_{1-14}$ may contribute to the observed reduction in cell viability when cells were treated with the Aβ$_{40}$ sample incubated with M-TTR and Zn(II), compared to the sample without Zn(II) (Fig. 1e). It is worth noting that additional hydrolytic products of Aβ (*e.g.*, Aβ$_{1-20}{}^{3+}$, Aβ$_{21-40}{}^{2+}$, Aβ$_{1-22}{}^{3+}$, Aβ$_{23-40}{}^{3+}$, and Aβ$_{34-40}{}^{+}$) were observed under both Zn(II)-treated and -untreated conditions (Fig. S19†), denoting that a minute quantity of Zn(II) remaining in the samples due to experimental limitations in purification processes may cause peptide hydrolysis. It is noteworthy that liquid chromatography coupled with MS (LC–MS) could not distinguish Aβ fragments detected under Zn(II)-treated conditions, possibly due to their similar retention time[61] and the detection limit of LC–MS under

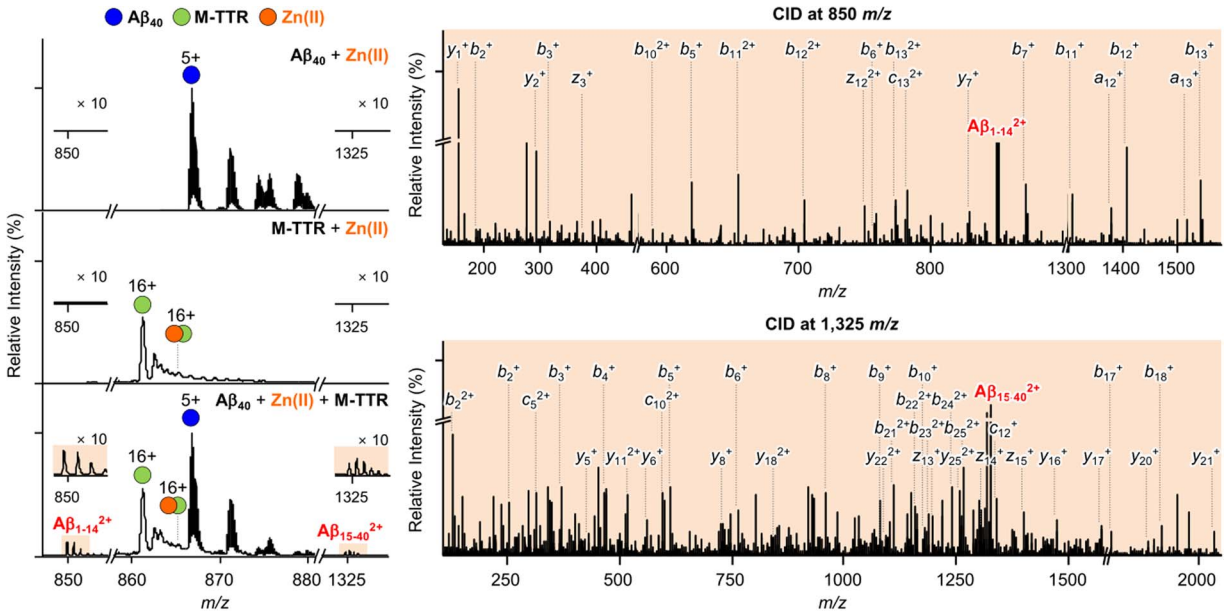

Fig. 4 Proteolytic activity of M-TTR against $A\beta_{40}$ in the presence of Zn(II). Aβ fragments [$A\beta_{1-14}^{2+}$ (850 *m*/*z*) and $A\beta_{15-40}^{2+}$ (1325 *m*/*z*)] were investigated by ESI–MS and ESI–MS^2. Charge states are marked above the peaks in the spectra. Conditions: [$A\beta_{40}$] = 100 μM; [M-TTR] = 100 μM; [$ZnCl_2$] = 100 μM; 20 mM ammonium acetate, pH 7.4; 37 °C; 24 h incubation; quiescent conditions. The samples were diluted 10-fold before injection into the mass spectrometer. The measurements were conducted in triplicate.

our experimental conditions (Fig. S20†). Overall results illustrate that M-TTR in the presence of Zn(II) promotes the proteolysis of $A\beta_{40}$ between His14 and Gln15, which potentially influences the aggregation and toxicity of $A\beta_{40}$.

Conclusions

Our studies shed light on the intricate interplay among M-TTR, Zn(II), and $A\beta_{40}$ in the context of AD pathology. We demonstrate that Zn(II) retains the anti-amyloidogenic ability of M-TTR, which spatially overlaps with Aβ in extracellular fluids,[6–9] against $A\beta_{40}$, albeit to a lesser extent. Through comprehensive investigations, we manifest the formation of a Zn(II)-promoted ternary complex involving M-TTR, $A\beta_{40}$, and Zn(II), which can tune the suppressive effect of M-TTR on the primary nucleation process and cytotoxicity of $A\beta_{40}$. Such binding also fosters the proteolytic cleavage of $A\beta_{40}$ and further redirects its aggregation and toxicity profiles. These interactions among M-TTR, $A\beta_{40}$, and Zn(II) reduce M-TTR's anti-amyloidogenic activity against $A\beta_{40}$ but allow it to maintain some inhibitory effect in the presence of Zn(II). Collectively, our findings offer a perspective on the collaborative roles of M-TTR and Zn(II) in modulating Aβ aggregation and toxicity. In the CSF, the presence of various metal ions and proteins capable of coordinating metal ions, in addition to M-TTR and Zn(II), suggests that dynamic interactions involved in Aβ-related pathology associated with AD may also extend to other metal ions (*e.g.*, copper)[41,62] and extracellular proteins (*e.g.*, human serum albumin).[63–66] Therefore, these findings contribute to our understanding of potential therapeutic targets and interventions for AD.[67–69]

Data availability

All experimental details and data supporting the findings of this study are available within the paper and its ESI.† The data are also available from the corresponding authors upon reasonable request.

Author contributions

Y. Y., J. H. K., and M. H. L. designed the research. Y. Y. performed biochemical and cell studies (cross-linking experiments with gel/western blot, ThT assay, and MTT assay) and the measurements of TEM, ESI–MS, and electronic Abs spectroscopy with data analyses and analyzed the LC–MS data. B. K. and J. H. K. prepared, purified, and characterized M-TTR. Y. H. K. and J. H. K. conducted 2D NMR studies with data analysis. M. K. conducted the ThT assay and the LC–MS analysis. Y. Y. and M. H. L. wrote the manuscript with input from all authors.

Conflicts of interest

There are no conflicts to declare.

Acknowledgements

This work was supported by the National Research Foundation of Korea (NRF) grants {Creative Research Initiative [RS-2022-NR070709] (M. H. L.); NRF-2020R1I1A2074335 (J. H. K.)} and the Institute for Basic Science of Korea [IBS-R034-D1 (Y. H. K.)], funded by the Korean government. M. K. thanks the Sejong Science Fellowship Grants (RS-2023-00214034).

Notes and references

1 L. Traxler, R. Lucciola, J. R. Herdy, J. R. Jones, J. Mertens and F. H. Gage, *Nat. Rev. Neurol.*, 2023, **19**, 434.
2 D. M. Walsh and D. J. Selkoe, *Nat. Rev. Neurosci.*, 2016, **17**, 251.
3 E. Karran and B. De Strooper, *Nat. Rev. Drug Discovery*, 2022, **21**, 306.
4 S. H. Han, J. C. Park and I. Mook-Jung, *Prog. Neurobiol.*, 2016, **137**, 17.
5 Y. Yi, J. Lee and M. H. Lim, *Trends Chem.*, 2024, **6**, 128.
6 J. N. Buxbaum, Z. Ye, N. Reixach, L. Friske, C. Levy, P. Das, T. Golde, E. Masliah, A. R. Roberts and T. Bartfai, *Proc. Natl. Acad. Sci. U. S. A.*, 2008, **105**, 2681.
7 X. Li, E. Masliah, N. Reixach and J. N. Buxbaum, *J. Neurosci.*, 2011, **31**, 12483.
8 X. Li, X. Zhang, A. R. A. Ladiwala, D. Du, J. K. Yadav, P. M. Tessier, P. E. Wright, J. W. Kelly and J. N. Buxbaum, *J. Neurosci.*, 2013, **33**, 19423.
9 A. L. Schwarzman, L. Gregori, M. P. Vitek, S. Lyubski, W. J. Strittmatter, J. J. Enghilde, R. Bhasin, J. Silverman, K. H. Weisgraber, P. K. Coyle, M. G. Zagorski, J. Talafous, M. Eisenberg, A. M. Saunders, A. D. Roses and D. Goldgaber, *Proc. Natl. Acad. Sci. U. S. A.*, 1994, **91**, 8368.
10 M. Alemi, C. Gaiteiro, C. A. Ribeiro, L. M. Santos, J. R. Gomes, S. M. Oliveira, P.-O. Couraud, B. Weksler, I. Romero, M. J. Saraiva and I. Cardoso, *Sci. Rep.*, 2016, **6**, 20164.
11 S. F. Gloeckner, F. Meyne, F. Wagner, U. Heinemann, A. Krasnianski, B. Meissner and I. Zerr, *J. Alzheimer's Dis.*, 2008, **14**, 17.
12 I. Elovaara, C. P. Maury and J. Palo, *Acta Neurol. Scand.*, 1986, **74**, 245.
13 E. M. Castano, A. E. Roher, C. L. Esh, T. A. Kokjohn and T. Beach, *Neurol. Res.*, 2006, **28**, 155.
14 M. G. Savelieff, G. Nam, J. Kang, H. J. Lee, M. Lee and M. H. Lim, *Chem. Rev.*, 2019, **119**, 1221.
15 J.-M. Suh, M. Kim, J. Yoo, J. Han, C. Paulina and M. H. Lim, *Coord. Chem. Rev.*, 2023, **478**, 214978.
16 K. P. Kepp, *Coord. Chem. Rev.*, 2017, **351**, 127.
17 S. Ayala, P. Genevaux, C. Hureau and P. Faller, *ACS Chem. Neurosci.*, 2019, **10**, 3366.
18 P. Faller and C. Hureau, *Dalton Trans.*, 2009, 1080.
19 Y. Miller, B. Ma and R. Nussinov, *Proc. Natl. Acad. Sci. U. S. A.*, 2010, **107**, 9490.
20 Y. Yi and M. H. Lim, *RSC Chem. Biol.*, 2023, **4**, 121.
21 S. Park, C. Na, J. Han and M. H. Lim, *Metallomics*, 2023, **15**, mfac102.
22 J. Han, Z. Du and M. H. Lim, *Acc. Chem. Res.*, 2021, **54**, 3930.
23 E. Nam, Y. Lin, J. Park, H. Do, J. Han, B. Jeong, S. Park, D. Y. Lee, M. Kim, J. Han, M.-H. Baik, Y.-H. Lee and M. H. Lim, *Adv. Sci.*, 2023, **11**, 2307182.
24 Z. Du, E. Nam, Y. Lin, M. Hong, T. Molnár, I. Kondo, K. Ishimori, M.-H. Baik, Y.-H. Lee and M. H. Lim, *Chem. Sci.*, 2023, **14**, 5340.
25 J. Han, J. Yoon, J. Shin, E. Nam, T. Qian, Y. Li, K. Park, S.-H. Lee and M. H. Lim, *Nat. Chem.*, 2022, **14**, 1021.
26 A. Abelein, A. Gräslund and J. Danielsson, *Proc. Natl. Acad. Sci. U. S. A.*, 2015, **112**, 5407.
27 L. Saelices, L. M. Johnson, W. Y. Liang, M. R. Sawaya, D. Cascio, P. Ruchala, J. Whitelegge, L. Jiang, R. Riek and D. S. Eisenberg, *J. Biol. Chem.*, 2015, **290**, 28932.
28 W. Colon and J. W. Kelly, *Biochemistry*, 1992, **31**, 8654.
29 T. R. Foss, R. L. Wiseman and J. W. Kelly, *Biochemistry*, 2005, **44**, 15525.
30 Z. H. Lai, W. Colon and J. W. Kelly, *Biochemistry*, 1996, **35**, 6470.
31 A. Quintas, D. C. Vaz, I. Cardoso, M. J. M. Saraiva and R. M. M. Brito, *J. Biol. Chem.*, 2001, **276**, 27207.
32 S. Susuki, Y. Ando, T. Sato, M. Nishiyama, M. Miyata, M. A. Suico, T. Shuto and H. Kai, *Amyloid*, 2008, **15**, 108.
33 L. d. C. Palmieri, L. M. T. R. Lima, J. B. B. Freire, L. Bleicher, I. Polikarpov, F. C. L. Almeida and D. Foguel, *J. Biol. Chem.*, 2010, **285**, 31731.
34 N. Marchi, V. Fazio, L. Cucullo, K. Kight, T. Masaryk, G. Barnett, M. Volgelbaum, M. Kinter, P. Rasmussen, M. R. Mayberg and D. Janigro, *J. Neurosci.*, 2003, **23**, 1949.
35 X. Jiang, C. S. Smith, H. M. Petrassi, P. Hammarstrom, J. T. White, J. C. Sacchettini and J. W. Kelly, *Biochemistry*, 2001, **40**, 11442.
36 J. Oroz, J. H. Kim, B. J. Chang and M. Zweckstetter, *Nat. Struct. Mol. Biol.*, 2017, **24**, 407.
37 R. Whelan, F. M. Barbey, M. R. Cominetti, C. M. Gillan and A. M. Rosická, *Transl. Psychiatry*, 2022, **12**, 473.
38 M. Biancalana and S. Koide, *Biochim. Biophys. Acta*, 2010, **1804**, 1405.
39 H. Tamano, R. Nishio, Y. Shakushi, M. Sasaki, Y. Koike, M. Osawa and A. Takeda, *Sci. Rep.*, 2017, **7**, 42897.
40 S. Vivekanandan, J. R. Brender, S. Y. Lee and A. Ramamoorthy, *Biochem. Biophys. Res. Commun.*, 2011, **411**, 312.
41 Y. Yi, W. Ryu, B. Kim, S. Muniyappan, K. Park, J. H. Kim and M. H. Lim, *ChemRxiv*, 2023, preprint, DOI: **10.26434/chemrxiv-2023-cx1zb**.
42 J. Du and R. M. Murphy, *Biochemistry*, 2010, **49**, 8276.
43 S. A. Ghadami, S. Chia, F. S. Ruggeri, G. Meisl, F. Bemporad, J. Habchi, R. Cascella, C. M. Dobson, M. Vendruscolo, T. P. J. Knowles and F. Chiti, *Biomacromolecules*, 2020, **21**, 1112.
44 G. Meisl, J. B. Kirkegaard, P. Arosio, T. C. Michaels, M. Vendruscolo, C. M. Dobson, S. Linse and T. P. J. Knowles, *Nat. Protoc.*, 2016, **11**, 252.
45 T. E. R. Werner, D. Bernson, E. K. Esbjorner, S. Rocha and P. Wittung-Stafshede, *Proc. Natl. Acad. Sci. U. S. A.*, 2020, **117**, 27997.
46 S. Linse, *Pure Appl. Chem.*, 2019, **91**, 211.
47 P. Arosio, R. Cukalevski, B. Frohm, T. P. J. Knowles and S. Linse, *J. Am. Chem. Soc.*, 2014, **136**, 219.
48 G. Meisl, X. Yang, E. Hellstrand, B. Frohm, J. B. Kirkegaard, S. I. Cohen, C. M. Dobson, S. Linse and T. P. J. Knowles, *Proc. Natl. Acad. Sci. U. S. A.*, 2014, **111**, 9384.

49 C. E. Sabel, J. M. Neureuther and S. Siemann, *Anal. Biochem.*, 2010, **397**, 218.
50 Y. Yi, Y. Lin, J. Han, H. J. Lee, N. Park, G. Nam, Y. S. Park, Y. H. Lee and M. H. Lim, *Chem. Sci.*, 2021, **12**, 2456.
51 N. Rezaei-Ghaleh, K. Giller, S. Becker and M. Zweckstetter, *Biophys. J.*, 2011, **101**, 1202.
52 J. Du, P. Y. Cho, D. T. Yang and R. M. Murphy, *Protein Eng., Des. Sel.*, 2012, **25**, 337.
53 D. T. Yang, G. Joshi, P. Y. Cho, J. A. Johnson and R. M. Murphy, *Biochemistry*, 2013, **52**, 2849.
54 G. D. Natale, G. Sabatino, M. F. M. Sciacca, R. Tosto, D. Milardi and G. Pappalardo, *Molecules*, 2022, **27**, 5066.
55 F. Lopez-Gallego, J. M. Guisan and L. Betancor, *Methods Mol. Biol.*, 2013, **1051**, 33.
56 M. A. Liz, S. C. Leite, L. Juliano, M. J. Saraiva, A. M. Damas, D. Bur and M. M. Sousa, *Biochem. J.*, 2012, **443**, 769.
57 I. E. Gouvea, M. Y. Kondo, D. M. Assis, F. M. Alves, M. A. Liz, M. A. Juliano and L. Juliano, *Biochimie*, 2013, **95**, 215.
58 C. Dammers, M. Schwarten, A. K. Buell and D. Willbold, *Chem. Sci.*, 2017, **8**, 4996.
59 K. Taş, B. D. Volta, C. Lindner, O. El Bounkari, K. Hille, Y. Tian, X. Puig-Bosch, M. Ballmann, S. Hornung, M. Ortner, S. Prem, L. Meier, G. Rammes, M. Haslbeck, C. Weber, R. T. A. Megens, J. Bernhagen and A. Kapurniotu, *Nat. Commun.*, 2022, **13**, 5004.
60 B. Murray, B. Sharma and G. Belfort, *ACS Chem. Neurosci.*, 2017, **8**, 432.
61 S. Du, E. R. Readel, M. Wey and D. W. Armstrong, *Chem. Commun.*, 2020, **56**, 1537.
62 L. Ciccone, C. Fruchart-Gaillard, G. Mourier, M. Savko, S. Nencetti, E. Orlandini, D. Servent, E. A. Stura and W. Shepard, *Sci. Rep.*, 2018, **8**, 13744.
63 T. S. Choi, H. J. Lee, J. Y. Han, M. H. Lim and H. I. Kim, *J. Am. Chem. Soc.*, 2017, **139**, 15437.
64 D. A. Bushinsky and R. D. Monk, *Lancet*, 1998, **352**, 305.
65 P. C. Johnson, W. O. Smith and B. Wulff, *J. Appl. Physiol.*, 1959, **14**, 859.
66 C. Cantarutti, M. C. Mimmi, G. Verona, W. Mandaliti, G. W. Taylor, P. P. Mangione, S. Giorgetti, V. Bellotti and A. Corazza, *Biomolecules*, 2022, **12**, 1066.
67 M. Ramesh, C. Balachandra, P. Andhare and T. Govindaraju, *ACS Chem. Neurosci.*, 2022, **13**, 2209.
68 Q. Cao, D. H. Anderson, W. Y. Liang, J. Chou and L. Saelices, *J. Biol. Chem.*, 2020, **295**, 14015.
69 M. Ramesh and T. Govindaraju, *Chem. Sci.*, 2022, **13**, 13657.